

Comparison between thaw-mounting and use of conductive tape for sample preparation in ToF-SIMS imaging of lipids in *Drosophila* microRNA-14 model

Minh Uyen Thi Le, Jin Gyeong Son, Hyun Kyoung Shon, Jeong Hyang Park, Sung Bae Lee, and Tae Geol Lee

Citation: *Biointerphases* **13**, 03B414 (2018); doi: 10.1116/1.5019597

View online: <https://doi.org/10.1116/1.5019597>

View Table of Contents: <https://avs.scitation.org/toc/bip/13/3>

Published by the American Vacuum Society

ARTICLES YOU MAY BE INTERESTED IN

Molecular depth profiling on rat brain tissue sections prepared using different sampling methods
Biointerphases **13**, 03B411 (2018); <https://doi.org/10.1116/1.5019611>

Toward multiplexed quantification of biomolecules on surfaces using time-of-flight secondary ion mass spectrometry
Biointerphases **13**, 03B413 (2018); <https://doi.org/10.1116/1.5019749>

Chemical imaging of aggressive basal cell carcinoma using time-of-flight secondary ion mass spectrometry
Biointerphases **13**, 03B402 (2018); <https://doi.org/10.1116/1.5016254>

NanoSIMS for biological applications: Current practices and analyses
Biointerphases **13**, 03B301 (2018); <https://doi.org/10.1116/1.4993628>

High resolution imaging and 3D analysis of Ag nanoparticles in cells with ToF-SIMS and delayed extraction
Biointerphases **13**, 03B410 (2018); <https://doi.org/10.1116/1.5015957>

Time of flight secondary ion mass spectrometry—A method to evaluate plasma-modified three-dimensional scaffold chemistry
Biointerphases **13**, 03B415 (2018); <https://doi.org/10.1116/1.5023005>

NEW

AVS Quantum Science
A high impact interdisciplinary journal for **ALL** quantum science



ACCEPTING SUBMISSIONS

Comparison between thaw-mounting and use of conductive tape for sample preparation in ToF-SIMS imaging of lipids in *Drosophila* microRNA-14 model

Minh Uyen Thi Le^{a)}

Department of Nano Science, University of Science and Technology (UST), Daejeon 34113, South Korea
and Center for Nano-Bio Measurement, Korea Research Institute of Standards and Science (KRISS),
Daejeon 34113, South Korea

Jin Gyeong Son^{a)} and Hyun Kyoung Shon

Center for Nano-Bio Measurement, Korea Research Institute of Standards and Science (KRISS),
Daejeon 34113, South Korea

Jeong Hyang Park and Sung Bae Lee

Department of Brain and Cognitive Sciences, Daegu Gyeongbuk Institute of Science and Technology (DGIST),
Daegu 42988, South Korea

Tae Geol Lee^{a),b)}

Department of Nano Science, University of Science and Technology (UST), Daejeon 34113, South Korea
and Center for Nano-Bio Measurement, Korea Research Institute of Standards and Science (KRISS),
Daejeon 34113, South Korea

(Received 14 December 2017; accepted 19 March 2018; published 30 March 2018)

Time-of-flight secondary ion mass spectrometry (ToF-SIMS) imaging elucidates molecular distributions in tissue sections, providing useful information about the metabolic pathways linked to diseases. However, delocalization of the analytes and inadequate tissue adherence during sample preparation are among some of the unfortunate phenomena associated with this technique due to their role in the reduction of the quality, reliability, and spatial resolution of the ToF-SIMS images. For these reasons, ToF-SIMS imaging requires a more rigorous sample preparation method in order to preserve the natural state of the tissues. The traditional thaw-mounting method is particularly vulnerable to altered distributions of the analytes due to thermal effects, as well as to tissue shrinkage. In the present study, the authors made comparisons of different tissue mounting methods, including the thaw-mounting method. The authors used conductive tape as the tissue-mounting material on the substrate because it does not require heat from the finger for the tissue section to adhere to the substrate and can reduce charge accumulation during data acquisition. With the conductive-tape sampling method, they were able to acquire reproducible tissue sections and high-quality images without redistribution of the molecules. Also, the authors were successful in preserving the natural states and chemical distributions of the different components of fat metabolites such as diacylglycerol and fatty acids by using the tape-supported sampling in microRNA-14 (miR-14) deleted *Drosophila* models. The method highlighted here shows an improvement in the accuracy of mass spectrometric imaging of tissue samples. © 2018 Author(s). All article content, except where otherwise noted, is licensed under a Creative Commons Attribution (CC BY) license (<http://creativecommons.org/licenses/by/4.0/>) <https://doi.org/10.1116/1.5019597>

I. INTRODUCTION

Biological and pharmaceutical research has aimed to discover fundamental biological mechanisms to reveal insights into human diseases and develop new drugs. Currently, a number of advanced quantitative technologies—high-performance liquid chromatography, liquid chromatography tandem-mass spectrometry (LC-MS/MS), and liquid chromatography-electrospray ionization tandem-mass spectrometry (LC-ESI-MS/MS)—are being widely used as analysis methods in research on biological mechanisms.^{1–6} However, although LC-MS is a highly sensitive and fast method for profiling compounds, it does not provide

information on the spatial distribution of target analytes on the sample surface.

Mass spectrometry imaging (MSI) can discriminate between drugs, their metabolites, and small molecular compounds (endogenous and pharmacological compounds), while simultaneously reporting their distributions on the sample surface. MSI is able to directly analyze the sample surface, typically by matrix-assisted laser deposition ionization, or by other ionization methods including secondary ionization mass spectrometry (SIMS) and desorption electrospray ionization. The MSI techniques can monitor the fundamental aspects of a variety of analytes, including metabolites, lipids, proteins, agrochemicals, and drugs in multiple tissue types.^{7–16} In the case of time-of-flight secondary ion mass spectrometry (ToF-SIMS) analysis, which is also used as an imaging tool to examine disease

^{a)}M. U. T. Le, J. G. Son, and T. G. Lee contributed equally to this work.

^{b)}Electronic mail: tglee@kriss.re.kr

biomarkers and the localization of therapeutic drugs, its advantages over other mass spectrometry (MS) analysis techniques lie in its increased spatial and mass resolutions.¹⁷ Notably, this ToF-SIMS analysis was achieved on an as-received sample, in a label-free manner without matrix deposition for ionization. MSI is a powerful technique for understanding the bio-distributions, accumulation, and metabolisms of drugs and diseases, and hence is being increasingly employed in pharmaceutical research. As evidenced in several studies,^{18–20} localization of biomolecules is most likely related to their biological functions. Hence, a deep understanding of the spatial distributions of the relevant biomolecular components, as well as the mechanistic effects of exogenous interferences in brain functions, plays a key role during drug discovery.^{21–24} Consequently, a proper sampling protocol is essential for obtaining the *ex vivo* molecular locations by mass spectrometry analysis.

To prepare MSI samples, the tissue sections are cut by using upright cryostat microtomes, after which the sample is transferred by brush onto an appropriate target plate (typically metal plate, ITO glass slide). The thaw-mounting method is typically used to adhere the sample onto the plate for MSI analysis. During the sampling process, the natural state of the sample can become altered due to folds, cracks, tears, or delocalization of the molecules in the tissue sections. Careful sampling is required to minimize analytical artifacts, and sampling can influence the outcome, especially when it is carried out by nonexperts. Recently, a few methods have been reported on for preparing MSI tissue samples as a way to overcome some issues. Acetate-film tape (3M, St. Paul, MN) was used as an adhesive for the tissue sample to prevent tearing or shattering of the sample during tissue sectioning, but this method is poor at maintaining the fine structures of the tissue and hinders ion detection due to the low conductivity of the acetate film.²⁵ The CryoJane tape-transfer system was also developed to facilitate sectioning of whole body tissues and bone samples,^{26,27} but the tape-transfer method requires several extra steps and the tissue section is likely to become contaminated by the adhesive portion of the CryoJane solution (from Leica system Co.) during UV cross-linking.²⁸ In short, the most important considerations regarding MSI sampling are maintaining the physical and chemical morphologies of the sample and avoiding the charge-effect of the tissue sample. For these reasons, the current report seeks to develop an optimal protocol for ToF-SIMS analysis of a biological sample. We describe a protocol for conductive tape-assisted cryosectioning, which significantly improves section quality and reduces the thermal effects and charge accumulation during ToF-SIMS analysis.

II. EXPERIMENT

A. Fly stock and sample preparation

The following *Drosophila melanogaster* lines were obtained from Bloomington Drosophila Stock Center: miR-14Δ1 (stock number: 33067) and w1118 (stock number: 3605). The latter was used as the control in this study. The

flies were raised in a standard medium (supplied by Biomax Co.) at 25 °C.

After culturing, the adult flies (one day after eclosion) were collected and loaded into a fly collar. The heads of the flies were kept at the same orientation. Thereafter, the fly collar was embedded in 10% gelatin (G1890, Sigma-Aldrich), which was subsequently frozen in liquid nitrogen and stored at -80 °C overnight. The frozen gelatin block containing the fly heads was detached from the fly collar, and sectioned using a cryo-microtome (Leica CM 3050S, Leica Biosystems Co., Germany) at -20 °C. The thickness was set to 10 μm in the dorsal direction. A section was mounted onto a precooled (-20 °C) stainless steel plate directly by using the thaw-mounting method (shown in Fig. 1) and the next section of the same head was mounted on another precooled (-20 °C) stainless steel plate by using the carbon tape-supporting method. A double-sided adhesive carbon tape (NEM tape, Nissin Co., Ltd., Japan) was used in the tape-supporting method. The carbon adhesive tape was placed onto the embedded-sample surface and rolled with a chilled roller to assure complete adhesion. As the cutting blade passed through the sample, the tape was gently lifted onto the chilled compartment of the cryo-microtome. Following the careful removal of the tape backing paper, the second adhesive surface was placed onto a conductive plate. In the thaw-mounting method, the fly head sections were cut and thaw-mounted on a clean stainless steel plate.²⁹ Samples could be stored in the deep-freezer before ToF-SIMS analysis.

In order to compare the two sample preparation methods—thaw-mounting and tape-mounting methods—we carried out three different ToF-SIMS analyses, including: (1) thaw-mounted sample measured at room temperature, (2) tape-mounted sample measured at room temperature, and (3) tape-mounted sample measured at -160 °C. For ToF-SIMS analysis at room temperature, the sectioned-sample on a stainless steel plate (-20 or -80 °C whether it was taken from a cryo-microtome or a deep-freezer) was again mounted onto a precooled (-80 °C) aluminum block and dried in a vacuum chamber for 3 h. Finally, the sectioned-sample substrate was transferred to the ToF-SIMS instrument for analysis at room temperature. For frozen-hydrated analysis at -160 °C, the tape-mounted sample on a stainless steel plate (-20 or -80 °C, depending on whether it was taken from a cryomicrotome or a deep-freezer, respectively) was mounted onto the precooled (-80 °C) heating/cooling sample holder G and was inserted into the load-lock chamber of the ToF-SIMS within a few seconds.⁴⁶ The cold finger was attached to the holder G after the vacuum level of the load-lock chamber was dropped to below about 1.0×10^{-5} mbar to avoid water condensation on the sample. After the sample holder G was cooled down for 1 h, it was transferred to the main chamber for analysis. During this process, the temperature of the sample holder G was maintained at -160 °C by making contact with the cold finger, which was supplied with liquid nitrogen in the load-lock and main chambers (ION-TOF cryo-SIMS system).

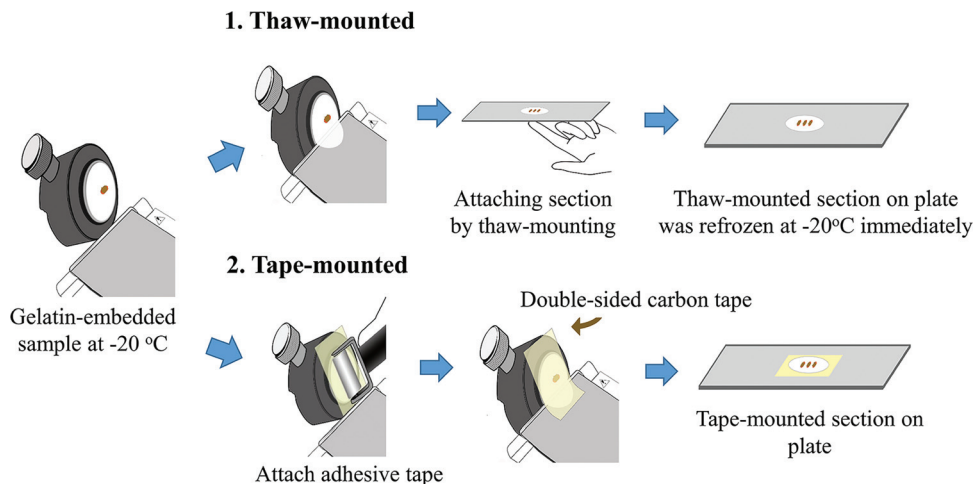


FIG. 1. Gelatin-embedded samples were prepared by two following methods, the thaw-mounting and tape-mounting methods.

B. ToF-SIMS analysis

All experiments were performed with a ToF-SIMS V instrument (ION-TOF GmbH, Germany) equipped with a bismuth liquid metal ion source. The secondary ions were generated by the 25-keV Bi_3^+ primary ion beam. In the experiments, a beam was set up to produce a beam current of approximately 0.1 pA with a beam size of approximately $3 \mu\text{m}$. For an image with a large field of view ($800 \times 800 \mu\text{m}^2$, 640×640 pixels), a stage-scan was performed in 3×3 patches in random mode. The primary ion dose density was set to 8×10^{11} ions/cm 2 . The frozen-hydrated analysis was carried out at a low temperature (-160°C) with an analysis area of $500 \times 500 \mu\text{m}^2$ (256×256 pixels).

Mass calibrations were internally performed by using the CH_3^+ , C_2H_3^+ , and C_3H_5^+ peaks for the positive ion spectra and CH^- , C_2H^- , and C_4H^- for the negative ion spectra. A low energy electron gun (10 V) was used during the analyses for charge compensation on the surface of the samples.

III. RESULTS AND DISCUSSION

A. Morphology of tissue section

In ToF-SIMS imaging analysis, the thaw-mounting method is a common method for mounting tissue sections onto target plates because this approach minimizes the risk of sample contamination. This technique provides quick and simple mounting (the protocol described in Fig. 1), but there are some drawbacks. First, varying degrees of disintegration and diffusion may occur in tissue sections depending on their levels of water,³⁰ which in turn vary according to the tissue type and disease stage.^{30–32} For example, cholesterol, mucopolysaccharides (long chains of sugar), and other extracellular components undergo some degrees of diffusion during thaw-mounting, which has been reported in previous literature.^{33–35} Moreover, the thaw-mounting method has been unable to produce subcellular resolution of tissues with small cells and high cell density, such as the

pituitary gland, lymph nodes, and even livers, but the subcellular images of these tissues were obtained using the tape-supporting method.^{29,36,37} To confirm this, we prepared samples using both the thaw-mounting and adhesive tape-supporting methods. The optical images of the fly brain tissues are shown in Figs. 2(a)–2(d).

The optic lobes of the adult *Drosophila* comprise major structures: the retina (Re), lamina (L), and medulla (Me) [Fig. 2(e)]. The retina structure of an adult fly includes a number of small ommatidia with rodlike structures. In the tape-supporting sampling procedure, we could easily observe the rodlike forms of the ommatidia in the retina (white triangle) [Fig. 2(a)], unlike in the thaw-mounted sample where they were blurred [Fig. 2(c)]. Moreover, the structures of some of the organs in the fly head, such as the retinas (Re) and laminas (L) became merged and showed evidence of horizontal wrinkling, as shown in Fig. 2(c). The thaw-mounted samples were characterized by the enlarged empty space between the tissue and embedding gelatin [marked by yellow arrows in Figs. 2(c) and 2(d)]. During thaw-mounting, adhesion of the tissue to the metal plate requires defrosting the section in order to avoid section detachment, which is normally done by using finger heat to defrost the tissue section. Unfortunately, this accelerates the accumulation of moisture on the tissue surface, thereby promoting the relocalization of some of the small molecules. In other words, this brief warming of the tissue, if only for seconds, results in ice crystal growth during the next refreezing step. In the refreezing process, the phase change of water to ice leads to the formation of ice crystals, which expand in volume and create sharp corners inside the cell, causing damage to the cell wall.^{37,38} By the end of this process, fluid that has escaped through the broken cell walls during the melting and refreezing process has led to tissue sections that have become wrinkled and diminished in size [Figs. 2(c) and 2(d)]. This process explains the reduction in the shape of the head section by $162 \mu\text{m}$ in length [Fig. 2(c)] as compared to the tape-supported sample [Fig. 2(a)]. In addition, there are

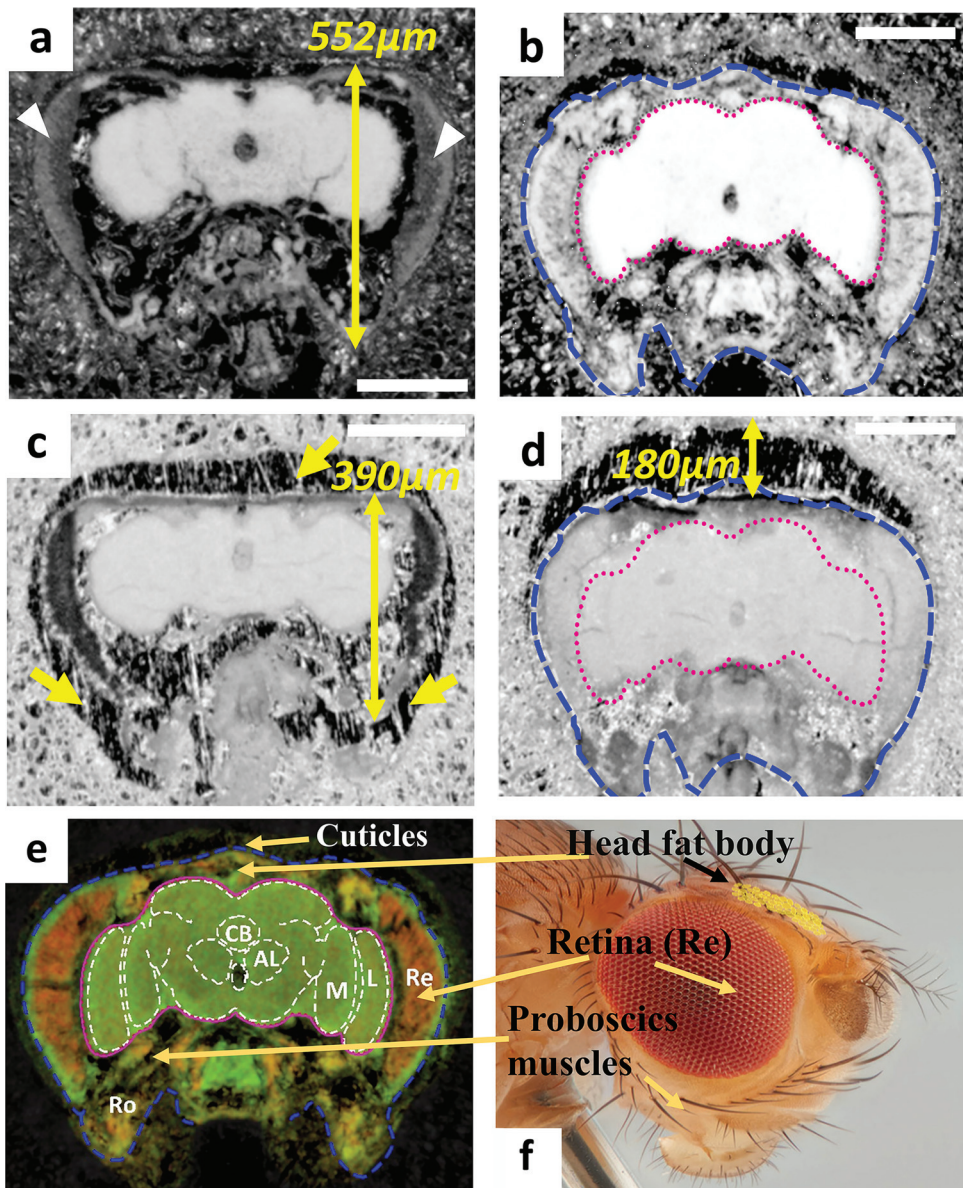


FIG. 2. Optical images of two different *Drosophila* model [transgenic flies—TH-GFP with red eyes (a), (c) and miRNA-14 (miR-14) flies with white eyes (b), (d)] brain tissue prepared by tape-supporting [(a), (b)] and thaw-mounting [(c), (d)] methods. (e) *Drosophila* brain diagram with cortex of brain (marked with magenta line); surrounding both the central brain and the optic lobes, retina (Re, in red), lamina (L), medulla (M), central body (CB), and antennal lobe (AL). *D. melanogaster* proboscis muscles (in Ro, rostrum) that manage the *Drosophila*'s feeding motions (Ref. 41). (f) Head fat body is within the head capsule (in yellow) (Ref. 51). The brain cortex (magenta dotted line) and head cuticles (blue dashed line at outer head) are marked in (b), (d), and (e). Size reduction (yellow arrows) and tissue moving of 180 μm in thaw-mounted samples were observed [(c), (d)]. Scale bar is 200 μm .

tissue shift of 180 μm in Fig. 2(d). The thaw-mounting method may result in a torn, wrinkled, or curled section due to the nonuniform temperature applied at the edges and center of the tissue section. In contrast, the tape-supporting method allows for easy mounting of the samples on the slides with a flat and smooth tissue surface, without distortion [Figs. 2(a) and 2(b)]. Using this method, we avoided breakage to or overlapping of the structures of some of the organs in the fly head such as the retinas (Re) and laminas (L), as this method removes the need to defrost the tissue section, thereby preventing the appearance of ice-crystals during the sampling process.

B. Migration of biomolecules in the fly brain

Using our sampling method, we investigated diacylglycerols (DAGs), triacylglycerols (TAGs), and fatty acid (FA) distributions on the fly head sections, which are known to be sensitive to temperature changes during sampling and measurements.³⁹ In addition, Cryo-ToF-SIMS measurement (referred to as frozen-hydrated analysis), a method to prevent delocalization of small molecules on the tissue surface of a sample,^{33,39} was carried out to examine the effects of temperature or drying process. Three sampling and analysis procedures—thaw-mounting, tape-supporting, and frozen-hydrated protocols—were applied to the

brain tissues of the miR-14 model fly to find the best sampling and analysis method for the *Drosophila* sample.

Previously, the signals at m/z 549.5 and 521.5 were assigned to the fragment of TAG (44:1) and DAG (30:1), respectively,⁴⁰ which are known to exist in large numbers^{39,40} on the head fat body and proboscis muscle regions (proboscis muscle 9 in rostrum)^{41,42}. The distinct ion signals of molecules at m/z 521.5 and m/z 549.5 showed that the different sample preparation methods affected molecular redistribution. Strong signals for these molecules were detected outside of the tissues in only the thaw-mounted samples [Figs. 3(c) and 3(f)], whereas the frozen-hydrated and tape-supported methods maintained their spatial information in the head fat body of *Drosophila* [Figs. 3(a), 3(b), 3(d), and 3(e)]. These results indicate that delocalization of biochemical molecules occurred due to slight thawing by finger heat or drying process during the thaw-mounting sampling.

In the negative ion images analysis, the ion signals of oleic acid (m/z 281.2) and palmitic acid (m/z 255.2) were strong near the head fat body and rostrum (Ro). Specifically, the palmitic acid signal at m/z 255.2 was strong in the retina (Re) and rostrum (Ro) areas, whereas the oleic acid signal at m/z 281.2 was strong in head cuticle (skull or head capsule of *Drosophila*). The ion signals of palmitic acid [$C_{16}H_{31}O_2^-$] in Figs. 3(g) and 3(h) and oleic acid [$C_{18}H_{33}O_2^-$] in Figs. 3(j) and 3(k) show a clear and significant spatial pattern that manifests as sharply denoted regions of cortex and glia surrounding the outer brain surface.^{43–45} In the thaw-mounted sample, however, two ion signals in Figs. 3(i) and 3(l) came not only from the fat body of the head, but also from the stainless steel plates. The overlay images of palmitic acid and oleic acid in

Figs. 3(m) and 3(n) clearly show their different local distributions, but in Fig. 3(o), these ion images are mostly overlaid at the same position, implying that the thaw-mounting sampling method caused the delocalization of small-molecule analytes on the tissue surface, unlike the other methods. After comparing the tape-supported analysis (at room temperature) and frozen-hydrated analysis (at -160°C), we could confirm that differences, especially in positive ion images, were minimal. As a result, we concluded that without finger heat and/or with excellent freeze-drying⁴⁶ during the tape-supporting sampling process, spatial molecular information in the tissue sections remained less affected.

In the frozen-hydrated analysis, unfortunately, we noted the presence of water cluster peaks in the negative spectra of the brain section, as already reported by Ewing and coworkers.³⁹ The condensation of small water ice crystals during the handling and transportation of frozen tissue into ToF-SIMS chamber could have an effect on the observations region of some molecules. In fact, a great deal of lipid information of the brain could be seen at around the m/z 700–800 region, but overlapping signals from the water cluster peaks made it difficult to resolve the peaks [Fig. S1(a)].⁵² For example, the peak at m/z 807.5 was overlaid with a water cluster in the frozen-hydrated sample, so that its image shows something blanketing the sample, compared with the clear image of the same m/z obtained from a tape-supported sample in Fig. S1(b). Another difficulty in the frozen-hydrated sample method is regards the analysis area, which is limited to $500 \times 500 \mu\text{m}^2$ because the stage scanning program is unable to operate with the heating and cooling holder (G) of the TOF-SIMS V equipment (ION-TOF GmbH).

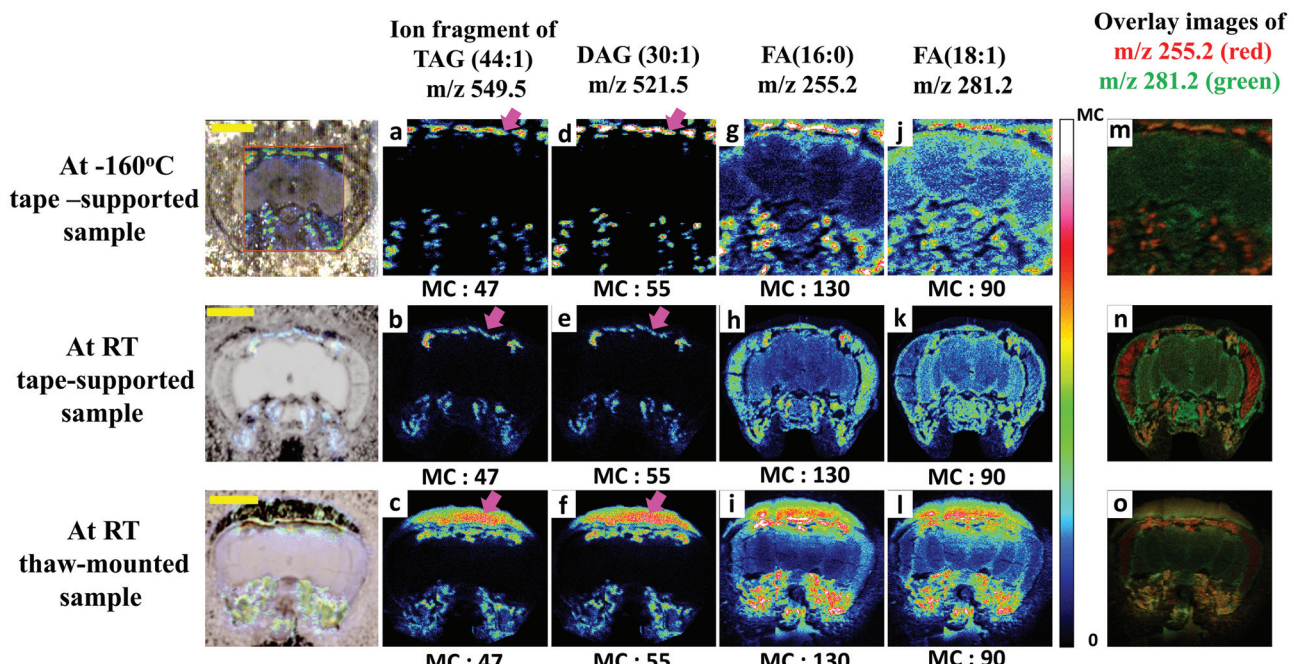


FIG. 3. Comparison of fly brains prepared by three different preparation and analysis procedures—tape-mounted at low temperature [(a), (d), (g), (j), and (m)], at room temperature [(b), (e), (h), (k), and (n)], and thaw-mounted at room temperature [(c), (f), (i), (l), and (o)]. The distributions of positive ions at m/z 549.5—ion fragment of TAG (44:1), and 521.5—DAG (30:1), respectively, and negative ions at m/z 281.2 [FA (18:1), oleic acid] and m/z 255.2 [FA (16:0), palmitic acid]. Scale bar is $200 \mu\text{m}$. MC stands for maximal counts.

Consequently, the *Drosophila* tissue samples that were prepared by the tape-supporting method were used to observe the whole *Drosophila* head (large analysis area).

C. Chemical distribution of miR-14 fly model

In *Drosophila*, previous reports have shown that the absence of miRNA-14 (miR-14) is correlated with defects related to apoptosis, stress response, lifespan, and metabolism.^{47,48} miR-14 affects the insulin-producing neurosecretory cells (IPCs) in the brain to control metabolism. Flies produce low levels of insulinlike peptides (Dilps) when they lack IPCs, leading to storage of excess fat in the head fat body. In the present study, the parallel tissue sections of wild-type and miR-14-lacking models were collected by carbon tape-supporting protocol, and ToF-SIMS analyses were carried out at room temperature to investigate the change in biochemical distributions between healthy and transgenic flies (Fig. 4).

Compared with the wild-type fly model, miR-14-lacking models showed few differences in the ion images of the phosphatidylcholine head-group (m/z 184.1) [in Figs. 4(a1) and 4(b1)], but the ion signal at m/z 495.5 dramatically increased in the salivary gland regions [white arrows in Figs. 4(a2) and 4(b2)]. This peak, previously known as DAG (28:0), was assigned to the fragment of TAG (40:0) according to previous MS/MS results⁴⁹ and our own electrospray ionisation collision-induced dissociation results of *Drosophila* lipid extracts (not shown). The overexpression of the miR-14-lacking model led to increased levels of TAG as well as the main circulating lipid DAG, and enlarged lipid droplets of *Drosophila*.^{47,49,50} Therefore, in the ToF-SIMS images, the signals and sizes of the regions related to the lipids such as TAG (40:0) [arrows in Figs. 4(a2) and 4(b2)] were stronger and larger in the miR-14 model flies than those in the wild-type flies. The fatty acid levels such as FA (18:2) (linoleic acid), FA (18:1) (oleic acid), and FA (18:0) (stearic

acid) [in Figs. 4(a3), 4(b3), 4(a4), 4(b4), 4(a5), and 4(b5)] at m/z 279.2, 281.2, and 283.2, respectively, were stronger in the miR-14 model flies. Based on the results from these tape-supported samples, we conclude that miR-14 mutants have increased levels of TAG and some fatty acids.

Delocalization of some molecules occurred during the thaw-mounting sampling procedure, making it difficult to distinguish between healthy and diseased flies (Fig. S2). For example, Fig. 4 from the tape-supported samples shows that the volume expansion of lipid droplet areas of the fragment ion of TAG (40:0) at m/z 495.5 [Figs. 4(a2) and 4(b2)] near the brain cortex of the miR-14 fly model is quite distinct, as compared with that of the wild-type model, whereas the thaw-mounted sample shows an uninterrupted area around the head body fat in Fig. S2b. These kinds of misleading or incorrect chemical information hinder our understanding of the pathways of disease development.

IV. SUMMARY AND CONCLUSIONS

The use of conductive double-sided adhesive carbon tape has been shown to enable the successful collection of small and fragile samples to surfaces compatible with ToF-SIMS analysis. The tape-supporting method can effectively preserve the distribution of small molecules in the same manner as that of the frozen-hydrated analysis (below -100°C). In addition, this method circumvents surface water interference, which is an issue in frozen-hydrated experiments. Improved sample mounting could reduce the variability in sample quality and increase improvement in accuracy and reproducibility of the tissue section. Based on ToF-SIMS results of carbon-tape supported samples, the miR-14 model flies suggests that lack of the miR-14 induced alterations in DAG levels and accumulation of the long-chain fatty acid. In summary, the protocols described here is a practical method of evaluating the different levels of lipids, metabolites, as a function of drug-feeding dose or disease processing, which

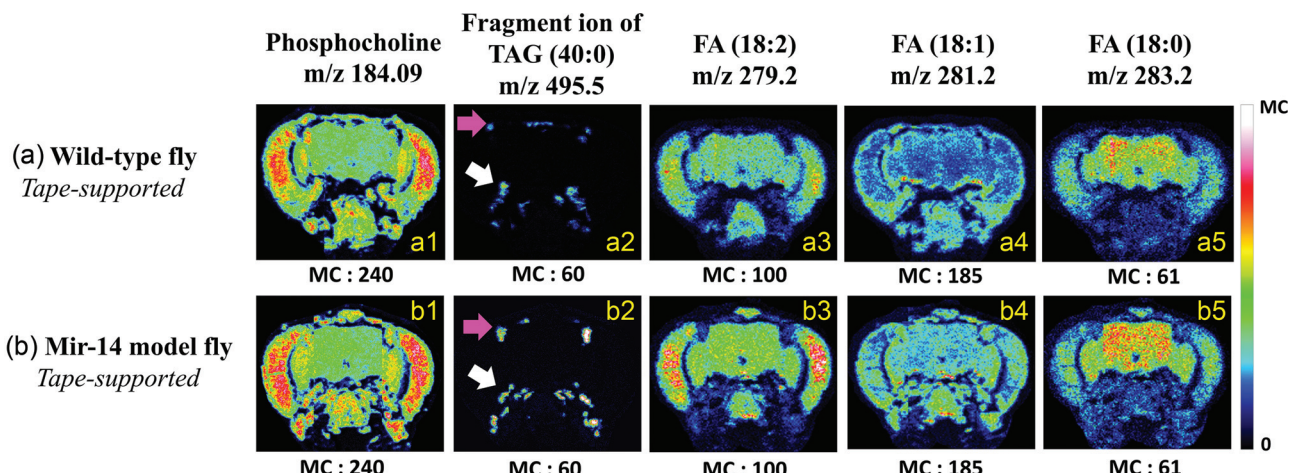


FIG. 4. ToF-SIMS images of the brains of wild-type (a) and miR-14 model flies (b). The samples were prepared by the tape-mounting method in positive ion mode at [(a1), (b1)] m/z 184.09—phosphocholine, [(a2), (b2)] and m/z 495.5—fragment of TAG (40:0). In the negative ion mode, there were [(a3), (b3)] m/z 279.2—FA (18:2) (linoleic acid), [(a4), (b4)] m/z 281.2—FA (18:1) (oleic acid), and [(a5), (b5)] m/z 283.2—FA (18:0) (stearic acid). MC stands for maximal counts.

would benefit both pharmaceutical and proteomic MSI research.

ACKNOWLEDGMENTS

The work was supported by the Development of Platform Technology for Innovative Medical Measurements Program (No. KRISS-2017-GP2017-0020) from the Korea Research Institute of Standards and Science, the Pioneer Research Program (No. NRF-2012-009541), the Bio & Medical Technology Development Program (No. NRF-2015M3A9D7029894), and the Global Frontier Project (No. H-GUARD_2013M3A6B2078962) of the National Research Foundation (NRF) funded by the Ministry of Science and ICT and Development of Nanotechnology-based Quantitative Surface Mass Spectrometric Platform Technique to Detect Low-mass Biomolecules funded by the MOTIE.

- ¹A. J. Ortiz, V. Cortez, A. Azzouz, and J. R. Verdu, *PLoS One* **12**, e0172202 (2017).
- ²Z. Z. Hauck, D. L. Feinstein, and R. B. van Breemen, *J. Anal. Toxicol.* **40**, 304 (2016).
- ³R. M. Borkar *et al.*, *Biomed. Chromatogr.* **30**, 1556 (2016).
- ⁴P. Sistik, R. Urinovska, H. Brozmanova, I. Kacirova, P. Silhan, and K. Lemr, *Biomed. Chromatogr.* **30**, 217 (2016).
- ⁵V. Kertesz, T. M. Weiskittel, M. Vavrek, C. Freddo, and G. J. Van Berkel, *Rapid Commun. Mass Spectrom.* **30**, 1705 (2016).
- ⁶W. Chen, L. Wang, G. J. Van Berkel, V. Kertesz, and J. Gan, *J. Chromatogr. A* **1439**, 137 (2016).
- ⁷M. E. Duenas, A. D. Feenstra, A. R. Korte, P. Hinnens, and Y. J. Lee, *Methods Mol. Biol.* **1676**, 217 (2018).
- ⁸M. Holzlechner, S. Reitschmidt, S. Gruber, S. Zeilinger, and M. Marchetti-Deschmann, *Proteomics* **16**, 1742 (2016).
- ⁹F. Marty *et al.*, *Anal. Chem.* **89**, 9664 (2017).
- ¹⁰R. L. Griffiths, E. C. Randall, A. M. Race, J. Bunch, and H. J. Cooper, *Anal. Chem.* **89**, 5683 (2017).
- ¹¹K. L. Fowble, K. Teramoto, R. B. Cody, D. Edwards, D. Guerrera, and R. A. Musah, *Anal. Chem.* **89**, 3421 (2017).
- ¹²M. Dilillo *et al.*, *Sci. Rep.* **7**, 603 (2017).
- ¹³M. R. L. Paine, P. C. Kooijman, G. L. Fisher, R. M. A. Heeren, F. M. Fernández, and S. R. Ellis, *J. Mater. Chem. B* **5**, 7444 (2017).
- ¹⁴D. Touboul and A. Brunelle, *Methods Mol. Biol.* **1203**, 41 (2015).
- ¹⁵M. L. Manier, J. M. Spraggins, M. L. Reyzer, J. L. Norris, and R. M. Caprioli, *J. Mass Spectrom.* **49**, 665 (2014).
- ¹⁶Y. Fujimura and D. Miura, *Metabolites* **4**, 319 (2014).
- ¹⁷J. S. Hammond, *Imaging Mass Spectrometry* (Springer, Tokyo, 2010), p. 235.
- ¹⁸F. Schmitz, E. B. Scherer, F. R. Machado, A. A. da Cunha, B. Tagliari, C. A. Netto, and A. T. Wyse, *Metab. Brain Dis.* **27**, 605 (2012).
- ¹⁹B. Lutz, *Endocannabinoids and Lipid Mediators in Brain Functions* (Springer International Publishing AG, Switzerland, 2017), p. 155.
- ²⁰A. J. L. Cooper and T. M. Jeitner, *Biomolecules* **6**, 16 (2016).
- ²¹K. D. Bruce, A. Zsombok, and R. H. Eckel, *Front. Endocrinol.* **8**, 60 (2017).
- ²²G. Khelashvili and H. Weinstein, *Biochim. Biophys. Acta* **1848**, 1765 (2015).
- ²³L. A. Becker *et al.*, *Nature* **544**, 367 (2017).
- ²⁴Y. H. Lin *et al.*, *Aging Cell* **13**, 755 (2014).
- ²⁵S. Khatib-Shahidi, M. Andersson, J. L. Herman, T. A. Gillespie, and R. M. Caprioli, *Anal. Chem.* **78**, 6448 (2006).
- ²⁶T. Kawamoto, *Arch. Histol. Cytol.* **66**, 123 (2003).
- ²⁷N. Zaima, N. Goto-Inoue, T. Hayasaka, and M. Setou, *Rapid Commun. Mass Spectrom.* **24**, 2723 (2010).
- ²⁸L. B. Martin, P. Nicolas, A. J. Matas, Y. Shinozaki, C. Catala, and J. K. Rose, *Nat. Protoc.* **11**, 2376 (2016).
- ²⁹S. H. Kim, J. Kim, Y. J. Lee, T. G. Lee, and S. Yoon, *J. Am. Soc. Mass Spectrom.* **28**, 1729 (2017).
- ³⁰Y. Dong, B. Li, S. Malitsky, I. Rogachev, A. Aharoni, F. Kaftan, A. Svatos, and P. Franceschi, *Front. Plant Sci.* **7**, 60 (2016).
- ³¹H. von Holst, X. Li, and S. Kleiven, *Acta Neurochir.* **154**, 1583 (2012).
- ³²N. S. Glaser, S. L. Wootton-Gorges, I. Kim, D. J. Tancredi, J. P. Marcin, A. Muir, and N. Kuppermann, *J. Pediatr.* **180**, 170 (2017).
- ³³S. Solé-Domènech *et al.*, *Acta Neuropathol.* **125**, 145 (2013).
- ³⁴H. Nygren, K. Börner, P. Malmberg, and B. Hagenhoff, *Appl. Surf. Sci.* **252**, 6975 (2006).
- ³⁵W. Stumpf, *Braz. J. Med. Biol. Res.* **31**, 197 (1998).
- ³⁶G. E. Duncan, *Advances in Metabolic Mapping Techniques for Brain Imaging of Behavioral and Learning Functions* (Springer, Netherlands, 1992), p. 151.
- ³⁷W. E. Stumpf, *Methods Cell Biol.* **13**, 171 (1976).
- ³⁸W. E. Stumpf and G. E. Duncan, *Methods Neurosci.* **3**, 35 (1990).
- ³⁹N. T. Phan, J. S. Fletcher, P. Sjovall, and A. G. Ewing, *Surf. Interface Anal.* **46**, 123 (2014).
- ⁴⁰N. T. N. Phan, M. Munem, A. G. Ewing, and J. S. Fletcher, *Anal. Bioanal. Chem.* **409**, 3923 (2017).
- ⁴¹O. Schwarz, A. A. Bohra, X. Liu, H. Reichert, K. VijayRaghavan, and J. Pielage, *eLife* **6**, e19892 (2017).
- ⁴²M. D. Gordon and K. Scott, *Neuron* **61**, 373 (2009).
- ⁴³V. Hartenstein, *Glia* **59**, 1237 (2011).
- ⁴⁴C. H. Lee, S. J. Blackband, and P. Fernandez-Funez, *Sci. Rep.* **5**, 8920 (2015).
- ⁴⁵M. K. DeSalvo, S. J. Hindle, Z. M. Rusan, S. Orng, M. Eddison, K. Halliwill, and R. J. Bainton, *Front. Neurosci.* **8**, 346 (2014).
- ⁴⁶H. K. Shon, S. H. Kim, S. Yoon, C. Y. Shin, and T. G. Lee, *Biointerphases* **13**, 03B411 (2018).
- ⁴⁷P. Xu, S. Y. Vernooy, M. Guo, and B. A. Hay, *Curr. Biol.* **13**, 790 (2003).
- ⁴⁸J. Varghese, S. F. Lim, and S. M. Cohen, *Genes Dev.* **24**, 2748 (2010).
- ⁴⁹B. R. Wilfred, W. X. Wang, and P. T. Nelson, *Mol. Genet. Metab.* **91**, 209 (2007).
- ⁵⁰K. D. Baker and C. S. Thummel, *Cell Metab.* **6**, 257 (2007).
- ⁵¹M. Tatar, S. Post, and K. Yu, *Trends Endocrinol. Metab.* **25**, 509 (2014).
- ⁵²See supplementary material at <https://doi.org/10.1116/1.5019597> for raw spectral data and detailed specifications.